The EMBO Journal vol.14 no.24 pp.6078–6086, 1995

DNA packaging orders the membrane of bacteriophage PRD1

Sarah J.Butcher, Dennis H.Bamford[1] and Stephen D.Fuller[2]

The Structural Biology Programme, European Molecular Biology Laboratory, Meyerhofstrasse 1, 69012 Heidelberg, Germany and [1]Department of Biosciences, Division of Genetics and Institute of Biotechnology, PO Box 56 (Viikinkari 5), University of Helsinki, FIN-00014 Helsinki, Finland

[2]Corresponding author

Bacteriophage PRD1 contains a linear dsDNA genome enclosed by a lipid membrane lying within a protein coat. Determination of the structure of the detergent-treated particle to 2 nm by cryo-electron microscopy and three-dimensional reconstruction has defined the position of the major coat protein P3. The coat contains 240 copies of trimeric P3 packed into positions of local 6-fold symmetry on a $T = 25$ lattice. The three-dimensional structures of the PRD1 virion and a DNA packaging mutant to a resolution of 2.8 nm have revealed specific interactions between the coat and the underlying membrane. The membrane is clearly visible as two leaflets separated by 2 nm and spanned by transmembrane density. The size of the coat does not change upon DNA packaging. Instead, the number of interactions seen between the protein shell and the membrane and the order of the membrane components increase. Thus the membrane of PRD1 plays a role in assembly which is akin to that played by the nucleocapsid in other membrane viruses.

Keywords: adenovirus/DNA packaging/enveloped virus/membrane organization/PRD1

Introduction

Membrane viruses have been studied as models for membrane traffic in cells. Work with eukaryotic viruses has established the need for a scaffold which organizes the membrane components. The protein composition of the viral membrane is tightly regulated, excluding host proteins. The role of the membrane in entry has also been elucidated for a number of viruses, however, only members of the alphaviruses have been characterized by icosahedral reconstruction (Fuller, 1987; Paredes *et al.*, 1993; Cheng *et al.*, 1995; Fuller *et al.*, 1995a). No X-ray structures of whole enveloped viruses have been solved, although some of their surface components have been characterized at the atomic level (Wilson *et al.*, 1981; Varghese *et al.*, 1983; Bullough *et al.*, 1994; Rey *et al.*, 1995).

PRD1 is a membrane-containing bacteriophage. Bacteriophages are useful model systems because they and their hosts are amenable to genetic and biochemical studies (Mindich and Bamford, 1988; Bamford *et al.*, 1995). PRD1 (Olsen *et al.*, 1974) is the type member of a commonly occurring group, the Tectiviridae (Francki *et al.*, 1991). PRD1 and PR4 are the best characterized of this group and are closely related (Bamford *et al.*, 1981; Myung *et al.*, 1994; Savilahti and Bamford, 1986) PRD1 infects Gram-negative bacteria which contain plasmids belonging to the P, W or N incompatability groups (Bradley, 1974; Olsen *et al.*, 1974; Bradley and Rutherford, 1975). These plasmids encode the receptor complex for the bacteriophage (Davis *et al.*, 1982; Kotilainen *et al.*, 1993; Pansegrau *et al.*, 1994), which also functions as a DNA transfer complex in conjugation (Dreiseikelmann, 1994; Lessl and Lanka, 1994). *Salmonella typhimurium* and *Escherichia coli* are amongst the common hosts of PRD1. The PRD1 genome is a linear double-stranded (ds) DNA molecule of 14 925 bp which has a covalently attached terminal protein on each 5′-terminus (Bamford *et al.*, 1983; Pakula *et al.*, 1989a,b; Bamford *et al.*, 1991). The genome is replicated by protein priming, as is the case for adenovirus and phage ϕ29 (reviewed in Salas, 1991).

PRD1 has an external protein shell surrounding an inner, protein-rich membrane which encloses the DNA (Figure 1). The external icosahedral coat of PRD1 contains the proteins P3 and P5. P3, the major coat protein, has a molecular weight of 43.1 kDa and P5, the minor coat protein, has a molecular weight of 34.3 kDa (Bamford and Bamford, 1990). These two proteins can be released as homo-oligomers by guanidine hydrochloride treatment of the virion, the rest of the proteins remaining associated with the membrane (Bamford and Mindich, 1982). Both the P3 and P5 oligomers are very stable, withstanding heating up to 70°C in the presence of 2% SDS (Mindich *et al.*, 1982b; Bamford and Bamford, 1990). Data from crystallized P3 (Stewart *et al.*, 1993b) and STEM mass measurements of the isolated P3 oligomer (Luo *et al.*, 1993b) indicate that the P3 oligomer is a trimer. Epitope mapping of P3 and truncated forms of P3 with a range of monoclonal antibodies has shown that the N-terminus is located within the virion and that the N-terminal 294 amino acids are sufficient for trimerization (Bamford *et al.*, 1993). Given the diameter of the virion and the number of copies of the major coat protein (Davis *et al.*, 1982), the T number for the virion has been estimated as lying between 13 and 37 (Stewart *et al.*, 1993b).

Underlying the external protein coat is the membrane. The membrane is complex, containing at least 15 distinct proteins. This is in contrast to the simpler membranes of some animal viruses, which typically contain a few protein species. The PRD1 membrane contains approximately equal amounts of protein and phosholipids (Davis *et al.*, 1982). The phospholipids are derived from the host cell membrane and contain 37% phosphatidlyglycerol, 56% phosphatidylethanolamine, and 5% cardiolipid (Davis *et al.*, 1982). The proteins are all encoded by the phage genome and at least 15 are thought to be either transmem-

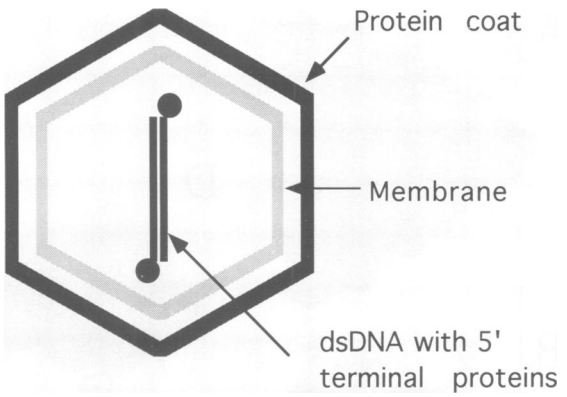

Fig. 1. A schematic diagram of PRD1. The icosahedral capsid of PRD1 consists of an external protein coat and a membrane. These enclose the linear ~15 kbp dsDNA genome and its 5'-terminally linked proteins.

brane or peripheral, judging by primary structure analysis (Bamford *et al.*, 1991) and their sensitivity to detergent, heat and pH (Caldentey *et al.*, 1993; Luo *et al.*, 1993a).

The life cycles observed for many bacteriophages involve a number of distinct stages. Many of these are characterized by morphologically recognizable capsid structures. When the nucleic acid is packaged, expansion is often seen from a procapsid to a mature capsid (Black, 1989; Fujisawa and Hearing, 1994). Such transitions during assembly are normally accompanied by increases in stability. The structural changes occurring during such expansions have been documented for P22 (Prasad *et al.*, 1993) and λ (Dokland and Murialdo, 1993). After a PRD1 infection ~20% of the isolated particles are empty (Bamford *et al.*, 1981). Empty particles can be pulse-chased during infection and have been shown to be precursors of the virion (Mindich *et al.*, 1982b). A nonsense mutation, *sus*1, which is defective in synthesis of the minor protein P9, prevents packaging of the genome, so that only empty particles are produced (Mindich *et al.*, 1982a,b). These have a similar protein and lipid composition to the wild-type empty particles, but the yield is greater and hence they are useful for structural studies. Empty particles isolated either during a normal wild-type infection or by the use of the *sus*1 nonsense mutation are less resistant to detergent treatment than the virions. This sensitivity allows shells of P3 to be isolated by SDS treatment of *sus*1 empty particles (Luo *et al.*, 1993a). In this study we have used cryo-electron microscopy (Adrian *et al.*, 1984) and three-dimensional reconstruction (Crowther, 1971; Fuller *et al.*, 1995b) to determine the structure of the virion, of the empty particle derived from the DNA packaging mutant and of the P3 shell. We show the organization of the P3 shell and the unusual structural rearrangements that occur in the membrane as a result of DNA packaging.

Results

Cryo-electron microscopy and image reconstruction

Electron micrographs of frozen hydrated PRD1 and *sus*1 are shown in Figure 2A. The capsids display a characteristic hexagonal outline, indicating their faceted nature.

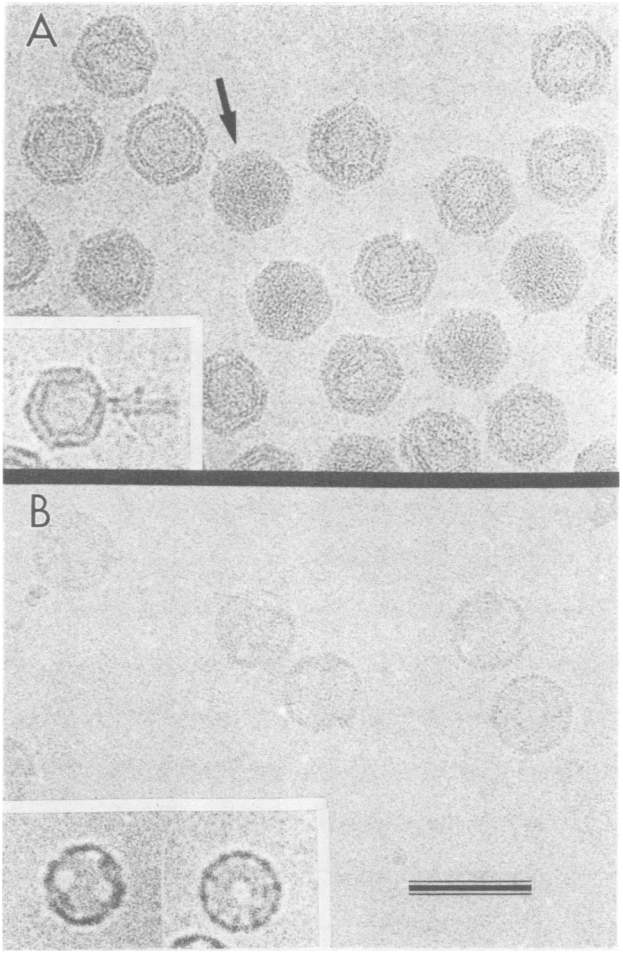

Fig. 2. Cryo-electron micrographs of PRD1 particles. (**A**) Wild-type PRD1 virions mixed with a preparation of the *sus*1 packaging mutant at 2 μm underfocus. The arrow points to a filled wild-type virion in which the internal density obscures the surface details. The packaging mutant produces empty patricles in which fine striations are seen in the outer shell. The membrane is also visible in these particles as an inner layer, which closely follows the outline of the outer shell in some particles. The inset shows a particle which has lost its DNA and has formed a tail from the membrane. (**B**) The packaging mutant after treatment with 1% SDS at 1 μm underfocus. The shell appears to be intact, but the membrane is missing. The inset shows two shells at 10 μm underfocus. In these highly defocussed images holes in the shell are emphasized. The particle on the left is close to a 2-fold orientation, the particle on the right is close to a 5-fold orientation. The scale bar represents 100 nm.

The smallest dimension of the virion is ~66 nm between opposing faces and the largest is ~74 nm between opposing vertices. PRD1 virions appear to be otherwise featureless. In the empty *sus*1 particle the contrast in the shell features is greater. The thin outer protein shell (~6 nm) and the internal membrane are seen distictly. Fine striations ~3.5 nm in width, arising from subunits of the shell, are visible at the edges of some particles. The contrast transfer function (CTF) at this defocus is maximal at 35 Å, thus accentuating features of this size. Only particles where the membrane adhered closely to the outer protein shell were used for the reconstruction. Wild-type filled PRD1 particles were mixed with *sus*1 empty particles so that a direct comparison could be made between the reconstructions, without the need for accurate CTF corrections. The *sus*1 reconstruction incorporated 33 particles to a resolution of 2.8 nm and the PRD1 reconstruction

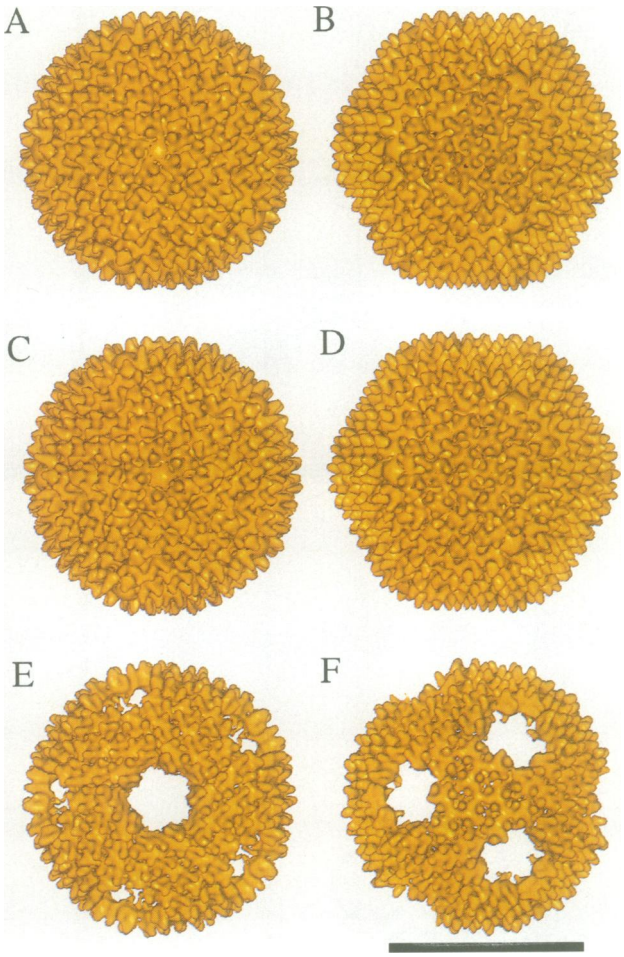

Fig. 3. Surface views of the reconstructions. The reconstructions are shown viewed down the 5-fold (A, C and E) and the 3-fold (B, D and F) axes. The front halves of the reconstructions are shown for the wild-type PRD1 (**A** and **B**), the empty particle (**C** and **D**) and the SDS-treated empty particle (**E** and **F**). Scale bar represents 50 nm.

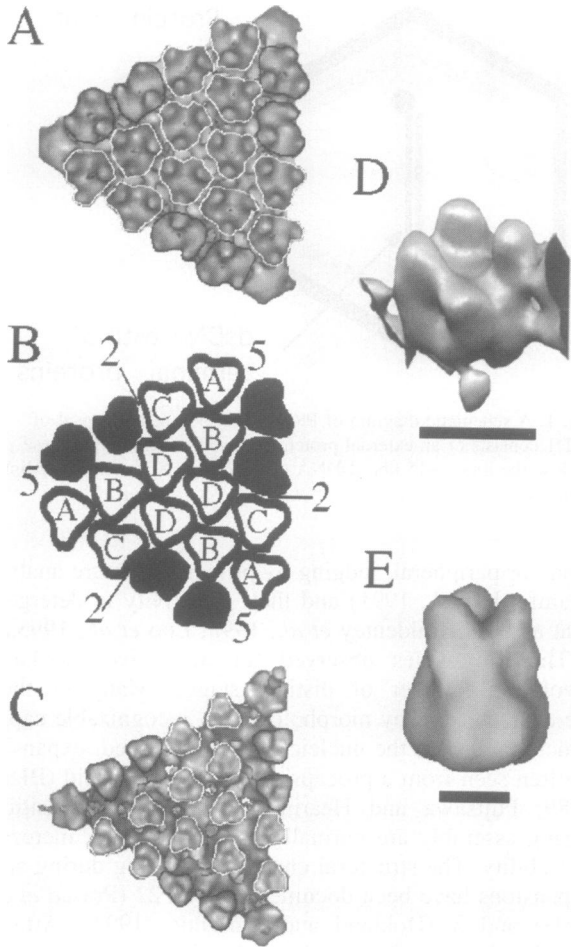

Fig. 4. The $T = 25$ arrangement of trimers in one facet. (**A**) A facet from the PRD1 virion reconstruction. Each of the 12 trimers from the same facet is outlined in white. Trimers from the neighbouring facets are marked in black. The length of one edge is 37 nm, measured between the 5-fold centres. (**B**) A schematic diagram of the trimers in a facet. The four quasi-equivalent trimer positions are marked A–D for the 12 trimers of one facet. The 5-fold (5) and 2-fold (2) axes are marked. The 3-fold axis lies in the centre of the face, between the D trimers. The trimers from adjoining facets are shown in black. (**C**) An equivalent facet from adenovirus for comparison. The length of one edge is 49 nm, measured between the 5-fold centres. Note the overall similarity with the PRD1 facet. However, the rotation of the trimers is different in the two structures. In the PRD1 facet the trimers around the 2-fold (C and trimer C' from the neighbouring facet) meet along their length. In adenovirus they meet corner to corner. (**D**) One B trimer which has been cut out of the SDS-treated empty particle reconstruction. This side view shows the three tower domains and the basal hexagonal domain, which is required for packaging into positions of quasi-6-fold symmetry. (**E**) A surface representation of the crystallographic density of the adenovirus hexon. Scale bars represent 5 nm in (D) and (E).

incorporated 26 particles to a resolution of 2.8 nm from a micrograph which was taken at 2 μm underfocus.

Figure 2B shows a micrograph of SDS-treated *sus*1 shells. These shells have a circular outline and do not contain an internal membrane (Luo *et al.*, 1993a). The inset shows two particles at 10 μm defocus, which emphasizes the presence of holes in the shell. The SDS-treated *sus*1 reconstruction incorporated 39 particles to a resolution of 2.0 nm from two micrographs which were taken at 1 μm underfocus.

Surface representations of the icosahedrally symmetrical PRD1 reconstruction are shown in Figure 3A (5-fold view) and B (3-fold view). The surface is organized on a '$T = 25$' symmetry lattice, with 240 trimers packed into positions of local 6-fold symmetry. This arrangement of the PRD1 external coat mirrors that of the '$T = 25$' adenovirus, as shown in Figure 4 (Stewart *et al.*, 1991, 1993a). In each facet, four copies of the trimeric P3 protein sit on the four distinct sets of six-coordinated positions of the $T = 25$ net. The five-coordinated position is occupied by a different structure.

The surface representations of the *sus*1 empty particle shown in Figure 3C and D appear to be very similar to those of the virion. However, the surface representations of the SDS-treated particles (Figure 3E and F), which retain only the major coat protein P3, reveal the holes on the 5-fold vertices. From this we can conclude that the trimers on the surface are formed from the major coat protein. The organization of the trimers is discussed in greater detail below.

Central cross-sections through the three structures reveal the layers of the structures and the major differences between them (Figure 5). The major coat protein shell of the SDS-treated particle reveals the extent of the P3 trimer density (Figure 5A). It is 9.1 nm long in the radial

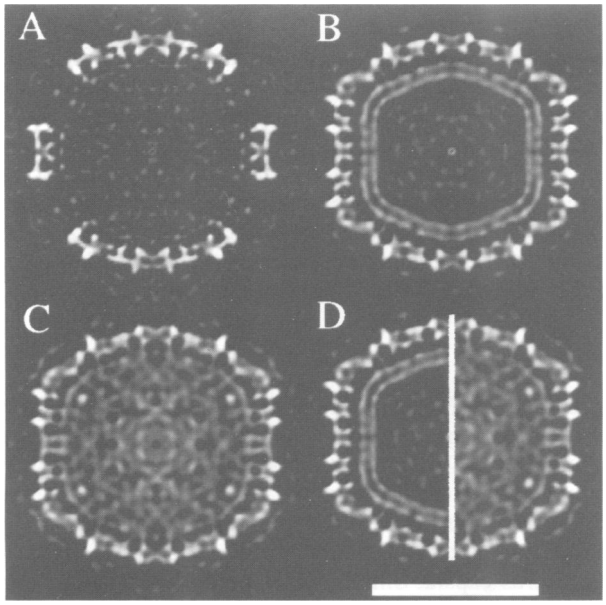

Fig. 5. Central sections of the reconstructions. Central sections perpendicular to the 2-fold axis are shown as continuous grey level representations, where high density is in white and low density solvent and lipid are in grey. (**A**) An SDS-treated *sus*1 particle. The shell is discontinuous due to the holes on the 5-fold vertices. (**B**) The *sus*1 central section has a complete protein shell and an internal membrane. Some connections are seen from the trimer to the membrane. Transmembrane regions are seen directly underneath these connections, as well as elsewhere in the membrane. (**C**) The central section of PRD1 has similar features, as well as a contribution from the DNA. (**D**) A direct comparison between the filled and empty particle. Scale bar represents 50 nm.

direction. The *sus*1 particle density (Figure 5B) reveals three layers of high density; the exterior protein shell and the outer and inner leaflets of the membrane. The bilayer is not spherical. It follows the curvature of the shell. Icosahedral membranes were also seen in reconstructions of alphaviruses (Fuller, 1987; Paredes *et al.*, 1993; Cheng *et al.*, 1995; Fuller *et al.*, 1995a).

Connections are seen between the trimers and the membrane. The virion cross-section (Figure 5C) also displays the outer protein shell and the inner membrane. The contrast of the inner bilayer is lower, however, than in the empty particle, due to the close proximity of the DNA. The connections from the trimers to the membrane are clearly evident here. There appears to be loosely organized material beneath the membrane, which is attributable to the DNA and its associated terminal proteins, but no distinct nucleocapsid is seen.

Structure and packing of the major coat protein

The asymmetric unit of the PRD1 capsid contains four quasi-equivalent types of trimers, denoted A–D in Figure 4. The homotrimer has a combined molecular weight of ~129 kDa (Bamford and Bamford, 1990). The trimer has three distal domains (towers) which are 3.4 nm in height and have an average peak-to-peak distance of 4.6 nm, as shown in Figure 4. The central third of the trimer is hexagonal, due to the presence of a second lower domain in each monomer. This second domain is evident in the trimers at the edge of the openings in the SDS-treated particle reconstruction (Figures 3E and F and 4D). The length of one side of the hexagonal base is 4.2 nm. The

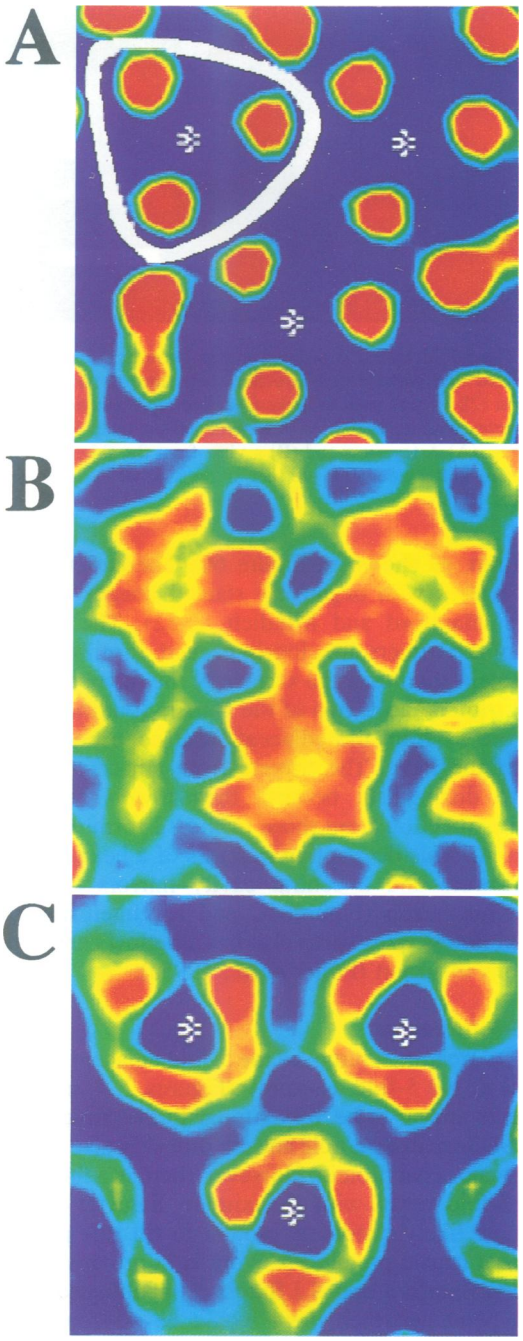

Fig. 6. Details of the trimer structure. The nature of the trimer is seen in the 2 nm resolution SDS-treated empty particle reconstruction. (A–C) Polar sections (Fuller *et al.*, 1995a) of the three D trimers about the 3-fold axis. The polar sections show the density between $\theta = -14.4°$ to $+14.4°$, $\phi = -33.8°$ to $-5°$. (**A**) At a radius of 33 nm, cutting through the towers of the trimer. An asterisk marks the position of the centre of each trimer. The towers from one trimer are ringed in white. (**B**) At a radius of 31 nm, cutting through the constricted region of the trimer, and also showing the six domains present in each trimer. (**C**) At a radius of 27 nm, showing the central cavity on the inside of the trimer. Blue denotes low density, red denotes high density.

hexagonal nature of the trimer can also be seen in the sections of the D trimers shown in Figure 6B. The centre of the trimer is constricted at the surface of the virion, but opens out again beneath this constriction. This creates a large cavity on the inside of the trimer with a diameter

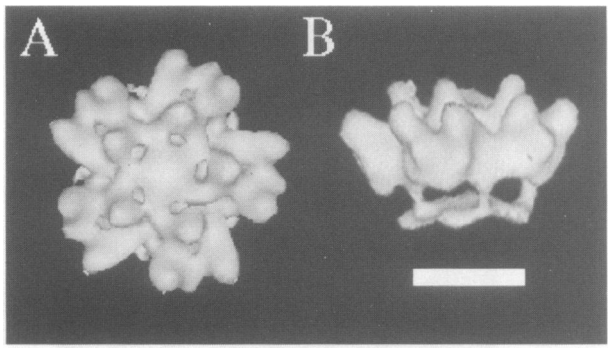

Fig. 7. The 5-fold vertex. A difference map between the *sus*1 and the SDS-treated *sus*1 particle reconstructions calculated to the same resolution (28 Å) was used to make a surface representation of the 5-fold vertex with its associated A trimers and the outer leaflet of the membrane. (**A**) A top view and (**B**) a view from the side. The connections to the membrane are seen in the side view. Scale bar represents 10 nm.

of 3.3 nm, as shown in Figure 6C. The structure of the trimer agrees with negatively stained images of isolated trimers (Bamford and Mindich, 1982). The hexagonal bases of the trimers are closely packed, forming a protective protein shell over the surface of the membrane. There are 12 trimers/facet, two of the trimers (outlined in black in Figure 4) from the adjacent facet contributing to the edge of the facet. The trimers from adjacent facets are easy to distinguish, because their towers face in the opposite direction from those of the 12 forming the facet (Figure 4). This description in terms of a hexagonal base, three towers and a central cavity mirrors that of the adenovirus hexon (Figure 4C and E). Interestingly, the Semliki Forest virus spike also has a hollow centre, which functions in fusion (Fuller *et al.*, 1995a).

The 5-fold vertex

The SDS treatment removes the 5-fold adjacent A trimers, as well as the 5-fold assembly (Figures 2, 4 and 7). The A trimers appear to be very similar to the trimers present in the SDS-treated particle and are probably also composed of the major coat protein. However, there is a flat structure at the 5-fold vertex with a maximum diameter of 5.2 nm. The most likely candidate protein to fill this position is the minor capsid protein P5. Work is in progress to verify this (J.K.Bamford and S.J.Butcher, unpublished data). If it is a pentamer, then there would be 60 copies of the monomer per virion, as opposed to the 39 copies proposed earlier (Davis *et al.*, 1982). The membrane relaxes into its more natural rounded curvature under the 5-fold vertex, where interactions with the membrane are less extensive.

Structural changes due to the presence of DNA

The reconstructions of the filled and the empty particle are very similar (cross correlation coefficient 0.9 to a resolution of 2.8 nm, of a maximal 1.0 for auto-correlation). This is a measure of the fidelity of the reconstructions. The external surfaces of the virion and the empty *sus*1 particles are nearly indistinguishable (Figure 3A–D). This is unusual for a dsDNA bacteriophage. Many of these have procapsids which undergo expansion during maturation, such as λ (Dokland and Murialdo, 1993) and P22 (Prasad *et al.*, 1993). However, there appear to be changes in the internal organization of the virion. The number of ordered connections which are visible between the major coat protein trimers and the membrane increases from one per trimer in the *sus*1 reconstruction to three per trimer in the virion (Figure 8). Transmembrane regions can be observed in both structures (Figures 5B and C and 8A and B). Within the membrane the order imposed by the surface lattice seems to be maintained in both particles (Figure 8); the density is better defined in the filled particle and may reflect a genuine increase in the icosahedral order of the membrane when it is in contact with DNA.

Discussion

Assembly of PRD1 appears to follow a middle path between that of the simple membrane viruses, where budding occurs via interaction of membrane proteins with an underlying capsid, and the complex viruses, where oligomeric units are linked by accessory proteins.

There are two fundamentally different ways of organizing a virus capsid. Simple viruses with low triangulation numbers, such as the $T = 3$ tomato bushy stunt virus, have relatively few distinct conformations of capsid protein and appear to switch between these conformations in a regular way. More complex viruses, including the $T = 25$ adenovirus, would require 25 different conformations of the capsid protein if they utilized the same scheme for achieving it as the simpler viruses. These more complex systems make use of sub-assemblies (for example the trimeric hexon which sits on the six coordinated positions of the capsid) and cementing proteins to overcome the need for the high number of conformations. The positions of these stabilizing proteins have been seen by disruption studies and difference imaging (Furcinitti *et al.*, 1989; Stewart *et al.*, 1991, 1993a).

The PRD1 capsid is made up of trimers of the major capsid protein P3 arranged in a $T = 25$ lattice (Figure 4) similar to that of adenovirus. The P3 trimer is one of the first intermediates in assembly. The trimer is a very stable building block which effectively reduces the number of units which need to be put together correctly from 720 to 240. When the P3 shell and empty particle reconstructions were compared at the same resolution no additional mass was observed that could be attributed to minor proteins in the shell except for that on the 5-fold vertex (Figure 7). The PRD1 membrane components probably act as a foundation for assembly, interacting with the coat proteins in construction of the capsid. Changes in the membrane components fulfil the same role as capsid expansion during DNA packaging of other phages.

P3 is essential for capsid formation (Mindich *et al.*, 1982a). The isolated P3 trimer has a ring-like appearance in negatively stained specimens, with a diameter of 6–7 nm (Bamford and Mindich, 1982). Both of these findings are consistent with our description of the trimer. Laser Raman spectroscopy of P3 indicates that the folding core of the protein is a β-sheet (~40% of the residues; Bamford *et al.*, 1990; Bamford and Bamford, 1990; R.Tuma, J.H.K.Bamford, D.H.Bamford, M.P.Russell and G.J. Thomas, in preparation). It has been estimated that there are at least two β-barrels within each P3 monomer. We have identified two domains in the monomer which may correspond to these β-barrels, the distal projecting domain and the hexagonal base domain. The trimer is a very

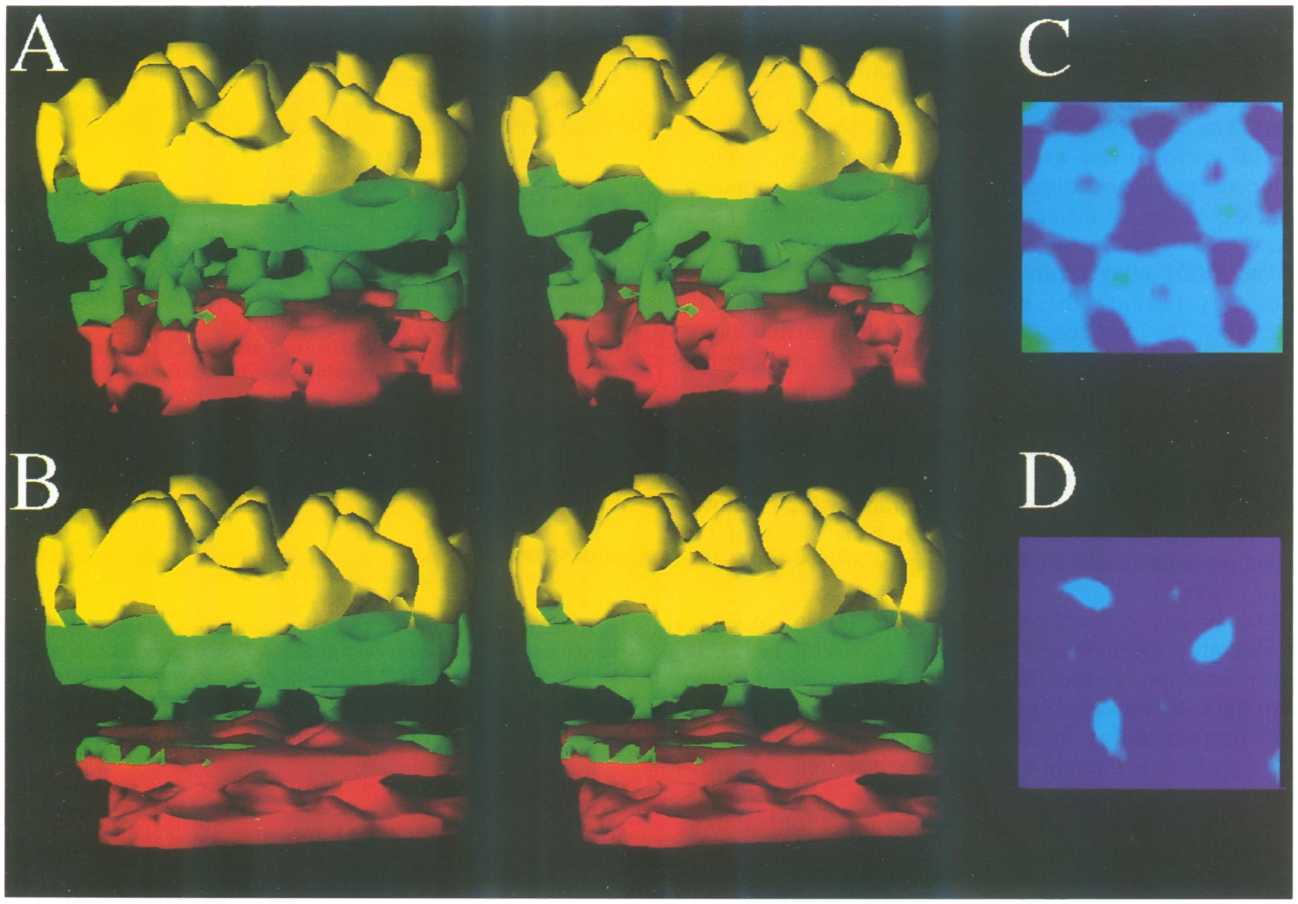

Fig. 8. Changes in membrane organization. (**A** and **B**) Stereo side views of the external protein coat and the membrane from a radius of 35 to 20 nm. The volume is taken from the 3-fold axis of either the filled particle (A) or the empty particle (B). The distal domain of the trimers is in yellow (radius 35–29 nm). The basal domain and legs to the membrane are shown in green (radius 29–24 nm). The membrane is shown in red (radius 24–20 nm). The number of visible connections that the major coat protein trimers make with the membrane increases from one per trimer to three per trimer after DNA packaging. This is also illustrated by panels (C) and (D). (**C** and **D**) Polar sections at a radius of 26 nm. In (C), from the filled particle, three connections are seen per trimer, whereas in (D), from the empty particle, only one connection is visible.

stable structure and the trimer contacts are robust, as most of the shell architecture appears not to have changed after SDS-treatment; so the interactions between monomers are probably extensive, as has been found for the adenovirus hexon trimer (Burnett *et al.*, 1985) and the bluetongue virus VP7 trimer (Grimes *et al.*, 1995).

The pseudohexagonal base allows the trimers to pack closely on the surface, with only an estimated 5% conformational change in main chain peptide bonds required for these lateral interactions to occur (R.Tuma, J.H.K. Bamford, D.H.Bamford, M.P.Russell and G.J.Thomas, in preparation). The D trimers around the 3-fold vertex appear to have a larger interaction surface than the other trimers. However, the interaction appears to be formed by the sub-domains of the trimers, rather than by an additional protein (Figure 6B), as in the case of adenovirus. Work is in progress to solve the crystal structure of the P3 protein (Stewart *et al.*, 1993b) so that we can fit this structure into the reconstruction of the P3 shell and define the subunit interactions more precisely, as has been done for adenovirus (Stewart *et al.*, 1993a) and for several other viruses (Cheng *et al.*, 1995; Grimes *et al.*, 1995; Ilag *et al.*, 1995).

The legs that extend from the shell to the membrane in the empty particle (one per trimer) are also present in the P3 shell, so it is likely that they are part of the P3 protein which interacts with the membrane. P3 is thought to be in contact with the membrane because it is readily cross-linked to the phosphatidylglycerol present in the membrane (Davis and Cronan, 1985).

Spectroscopy indicates that the DNA and the lipid head groups of the membrane interact tightly (R.Tuma, J.H.K.Bamford, D.H.Bamford, M.P.Russell and G.J. Thomas, in preparation). The close contact of the DNA and the membrane is obvious in our micrographs and reconstructions from the lack of contrast between the membrane and the DNA.

The virion is more stable than the empty particle (Luo *et al.*, 1993a). Unlike many dsDNA-containing bacteriophages, this increase in stability is not associated with a major change in capsid shape coincident with DNA packaging. The only differences that could be attributed to packaging occurred in the membrane and in associated structures (Figures 5B–D and 8). The number of visible, ordered connections from P3 to the membrane tripled (Figure 8). It is unlikely that this additional density is from a novel protein added during packaging, as the only additional structural proteins in the virion are the minor packaging protein P9 and the terminal protein (Bamford *et al.*, 1995). Rather, it may reflect a conformational

change, which has also been detected by laser Raman spectroscopy as an increase in the α-helical signal of the membrane-associated proteins (R.Tuma, J.H.K.Bamford, D.H.Bamford, M.P.Russell and G.J.Thomas, in preparation). The sensitivity of the *sus*1 membrane (Luo *et al.*, 1993a) could be due to disordered contacts between the outer coat and the membrane in the *sus*1 particles compared with the virion or differences in the accessibility of the membrane to detergents in the two particles.

The PRD1 bilayer can be removed by SDS treatment without perturbing the shape of the remaining shell. Therefore, the icosahedral shape of the protein-rich membrane is imposed by its interactions with the shell, rather than being intrinsic to the membrane. Where there are connections to the shell (under each trimer), the radius of curvature of the membrane is greater than in their absence (underneath the 5-fold vertex). This recapitulates the observations of the alphavirus membrane, which follows the curvature of the nucleocapsid and the skirts of the spike proteins (Fuller, 1987; Cheng *et al.*, 1995; Fuller *et al.*, 1995a).

Membranes of enveloped viruses function in entry and in assembly (Simons and Fuller, 1987; White, 1992). In many enveloped viruses the envelope is required for fusion with the cell endosomal membrane in order to release the nucleocapsid during infection. The close packing of the spike proteins is thought to control the envelope composition in assembly. A further interaction with the nucleocapsid via transmembrane regions is required for budding.

The mechanism of PRD1 entry remains unclear, however, comparison with adenovirus is suggestive. The adenovirus 5-fold vertex is a functional site in the capsid, where virus uncoating during infection is initiated (Greber *et al.*, 1993). The trimer–trimer contacts between the 5-fold adjacent trimers in PRD1 (labelled A in Figure 4) and their neighbours are weaker than the other trimer–trimer contacts, resulting in their loss from the structure after SDS treatment. In PRD1 the membrane forms a tube through a vertex of the coat (Figure 2A, insert) for delivery of the DNA (Bamford and Mindich, 1982; Luo *et al.*, 1993a; Bamford *et al.*, 1995). The dimensions of this tube and of the hole formed in the SDS-treated protein shell are similar (outer diameter ~20 nm).

During the assembly of PRD1 the cytoplasmic membrane containing the viral proteins acts as an assembly site for the coat proteins, which then interact laterally, excluding host proteins. The capsid then buds into the cytoplasm, in a manner analogous to that seen for the assembly of clathrin-coated pits (Bamford *et al.*, 1995).

PRD1 represents a novel combination of structural elements seen in other enveloped viruses (Paredes *et al.*, 1993; Cheng *et al.*, 1995; Fuller *et al.*, 1995a) and non-enveloped viruses (Stewart *et al.*, 1991). The structure illustrates the importance of lateral interactions in viral and membrane assembly. The similarities to other virus structures have functional implications which we are pursuing with the combination of genetic, biochemical and structural techniques used here.

Materials and methods

Preparation of virus stocks

The wild-type PRD1 (Olsen *et al.*, 1974) was grown on the non-suppressor host *Salmonella enteritica* var. *typhimurium* LT2 DS88 (Bamford and Bamford, 1990) containing the plasmid pLM2 (Mindich *et al.*, 1976) at 37°C. The bacteriophage was purified essentially according to Walin *et al.* (1994). Briefly, exponentially growing cultures of DS88 in LB broth were infected at a cell density of 1×10^9 c.f.u./ml using a multiplicity of infection of five. Incubation was continued until lysis occurred. The cell debris was removed by low speed centrifugation (Sorvall GS3 rotor, 8000 r.p.m., 20 min, 4°C) and the bacteriophages concentrated from the resulting supernatant by the addition of 10% PEG 6000 and 0.5 M NaCl (Bamford *et al.*, 1981). The concentrated phages were then purified on 5–20% linear sucrose gradients in 20 mM Tris–HCl, pH 7.5 (24 000 r.p.m., 50 min, 15°C, Beckman SW28). This allows the separation of empty and filled particles. The virus band was then applied to a MemSep DEAE cartridge (Millipore Corp.) and eluted with a NaCl gradient in 20 mM Tris–HCl, pH 6. The protein concentration was determined by the Bio-Rad protein assay according to the manfacturer's instructions, using bovine serum albumin as the standard. The preparation was stored on ice until required.

The PRD1 nonsense mutation *sus*1 in gene IX prevents DNA packaging (Mindich *et al.*, 1982a,b). *Salmonella enteritica* var. *typhimurium* PSA was used as the suppressor and DS88 as the non-suppressor host for *sus*1 propagation. Purification was as for wild-type PRD1.

SDS treatment

SDS treatment was carried out essentially according to Luo *et al.* (1993a). The purified *sus*1 empty particles were treated with 1% SDS at a final protein concentration of 1.5 mg/ml for 15 min at 25°C. The treated particles were then sedimented in a 5–20% linear sucrose gradient in 10 mM Tris–HCl, pH 7.5 (30 000 r.p.m., 95 min, 15°C, Beckman SW41). The light scattering band was harvested and analysed by SDS–PAGE (Olkkonen and Bamford, 1989).

Electron microscopy

Microscopy was performed essentially according to Adrian *et al.* (1984). The specimen was applied to a holey carbon film (Fukami and Adachi, 1965) on a 200 mesh copper grid. The grid was blotted with filter paper and vitrified by plunging it into ethane slush using a guillotine-like device. The vitrified specimen was then transferred to a cooled Gatan 626 cryostage maintained at a temperature of <–170°C. Electron micrographs were recorded under low dose conditions on a Philips CM200 electron microscope, fitted with an anti-contaminator and a field emission gun, operating at 200kV. Focal series were typically recorded at 2 and 4 μm underfocus at a magnification of 38 000. The magnification of the negatives was calibrated using Semliki Forest virus (70 nm diameter) as an internal standard. The closest to focus image was recorded first. Negatives were developed in full strength D19 for 12 min.

Image processing

Negatives were assessed on an optical diffractometer for lack of astigmatism and drift. Suitable negatives were scanned on a Perkin Elmer PDS 1010M flatbed microdensitometer at a step size of 26 μm, corresponding to 0.67 nm in the images. Wild-type and the empty *sus*1 particles were selected from the same negative. A background ramp was subtracted from the images before they were masked and centred interactively. Image processing (selection, ramping and masking) was performed using the programs EMICO (Metcalf *et al.*, 1991) and SPIDER (Frank *et al.*, 1981). Orientations and centres were determined and refined using the common lines procedure (Crowther *et al.*, 1970; Crowther, 1971; Fuller, 1987; Fuller *et al.*, 1995b). The furthest from focus images of the SDS-treated particles were refined initially, as the holes in the shell made the orientation search very effective. The particle phase residuals became strongly handed once they were refined to at least 3.3 nm. This allowed exclusion of particles if the hand was inconsistent with that of the other particles (Stewart *et al.*, 1991; Dokland and Murialdo, 1993; Fuller *et al.*, 1995b). The maps were calculated at 28 Å for the filled and empty particles and 20 Å for the P3 shell. All the eigenvalues were >10, showing that reciprocal space was adequately sampled. Further refinement and checking of the model was performed using the polar Fourier transform method (Cheng *et al.*, 1994, 1995; Baker and Cheng, 1995; Fuller *et al.*, 1995b). This also enabled us to find the initial orientations of both the empty and filled particles by using the P3 shell as a model. More complete descriptions of the programs and supplementary information can be obtained from http://www.embl-heidelberg.de/ExternalInfo/fuller/EMBL_Virus_Structure.html.

Acknowledgements

Dr Jaana Bamford (Helsinki) is thanked for her skilful preparation of the virions and the *sus*1 particles. Patricia Buck (EMBL) is thanked for providing samples of Semliki Forest virus. Brent Gowen (EMBL) is thanked for doing some of the electron microscopy. Dr George Thomas Jr and his group (Department of Cell Biology and Biophysics, School of Biological Sciences, University of Missouri, Kansas City, MO) are thanked for sharing unpublished results and critical reading of the manuscript. Drs Peter Metcalf (EMBL), Timothy Baker and Holland Cheng (Structural Studies, Department of Biological Sciences, Purdue University, West Lafayette, IN) are thanked for generously supplying their programs. S.J.B. was supported by a European Union Science grant (ERBSC1*CT000735) awarded to S.D.F. D.H.B. was supported by the Finnish Academy of Sciences.

References

Adrian,M., Dubochet,J., Lepault,J. and McDowall,A.W. (1984) Cryo-electron microscopy of viruses. *Nature*, **308**, 32–36.

Baker,T.S. and Cheng,R.H. (1995) A model-based approach for determining orientations of biological macromolecules imaged by cryo-electron microscopy. *J. Struct. Biol.*, in press.

Bamford,D.H. and Mindich,L. (1982) Structure of the lipid-containing bacteriophage PRD1: disruption of wild-type and nonsense mutant phage particles with guanidine hydrochloride. *J. Virol.*, **44**, 1031–1038.

Bamford,D.H., Rouhiainen,L., Takkinen,K. and Söderlund,H. (1981) Comparison of the lipid-containing bacteriophage PRD1, PR3, PR4, PR5 and L17. *J. Gen. Virol.*, **57**, 365–373.

Bamford,D.H., McGraw,T., Mackenzie,G. and Mindich,L. (1983) Identification of a protein bound to the termini of bacteriophage PRD1 DNA. *J. Virol.*, **47**, 311–316.

Bamford,D.H., Bamford,J.K.H., Towse,S.A. and Thomas,G.J.J. (1990) Structural study of the lipid-containing bacteriophage PRD1 and its capsid and DNA components by laser Raman spectroscopy. *Biochemistry*, **29**, 5982–5987.

Bamford,D.H., Caldentey,J. and Bamford,J.K.H. (1995) Bacteriophage PRD1: a broad host range dsDNA Tectivirus with an internal membrane. *Adv. Virus Res.*, **45**, 281–319.

Bamford,J.K. and Bamford,D.H. (1990) Capsomer proteins of bacteriophage PRD1, a bacterial virus with a membrane. *Virology*, **177**, 445–51.

Bamford,J.K., Hänninen,A.L., Pakula,T.M., Ojala,P.M., Kalkkinen,N., Frilander,M. and Bamford,D.H. (1991) Genome organization of membrane-containing bacteriophage PRD1. *Virology*, **183**, 658–676.

Bamford,J.K., Luo,C., Juuti,J.T., Olkkonen,V.M. and Bamford,D.H. (1993) Topology of the major capsid protein P3 of bacteriophage PRD1: analysis using monoclonal antibodies and C-terminally truncated proteins. *Virology*, **197**, 652–658.

Black,L.W. (1989) DNA packaging in dsDNA bacteriophages. *Annu. Rev. Microbiol.*, **43**, 267–292.

Bradley,D.E. (1974) Adsorption of bacteriophages specific for *Pseudomonas aeruginosa* R factors RP1 and R1822. *Biochem. Biophys. Res. Commun.*, **57**, 893–900.

Bradley,D.E. and Rutherford,E.L. (1975) Basic characterization of a lipid-containing bacteriophage specific for plasmids of the P, N and W incompatability groups. *Can. J. Microbiol.*, **21**, 152–163.

Bullough,P.A., Hughson,F.M., Skehel,J.J. and Wiley,D.C. (1994) The structure of the influenza haemagglutinin at the pH of membrane fusion. *Nature*, **371**, 37–43.

Burnett,R.M., Grütter,M.G. and White,J.L. (1985) The structure of the adenovirus capsid. I. An envelope model of hexon at 6 Å resolution. *J. Mol. Biol.*, **185**, 105–123.

Caldentey,J., Luo,C. and Bamford,D.H. (1993) Dissociation of the lipid-containing bacteriophage PRD1: effects of heat, pH, and sodium dodecyl sulfate. *Virology*, **194**, 557–563.

Cheng,R.H., Reddy,V.S., Olson,N.H., Fisher,A.J., Baker,T.S. and Johnson,J.E. (1994) Functional implications of quasi-equivalence in a T = 3 icosahedral animal virus established by cryo-electron microscopy and X-ray crystallography. *Structure*, **2**, 271–282.

Cheng,R.H., Kuhn,R.J., Olson,N.H., Rossmann,M.G., Choi,H.-K., Smith,T.J. and Baker,T.S. (1995) Nucleocapsid and glycoprotein organization in an enveloped virus. *Cell*, **80**, 621–630.

Crowther,R.A. (1971) Procedures for three-dimensional reconstruction of spherical viruses by Fourier synthesis from electron micrographs. *Phil. Trans. R. Soc. Lond. B*, **261**, 221–230.

Crowther,R.A., DeRosier,D.J. and Klug,A. (1970) The reconstruction of a three-dimensional structure from projections and its application to electron microscopy *Proc. R. Soc. Lond. A*, **317**, 319–340.

Davis,T.N. and Cronan,J.E. (1985) An alkyl imidate labelling study of the organization of phospholipids and proteins in the lipid-containing bacteriophage PR4. *J. Biol. Chem.*, **260**, 663–671.

Davis,T.N., Muller,E.D. and Cronan,J.E. (1982) The virion of the lipid-containing bacteriophage PR4. *Virology*, **120**, 287–306.

Dokland,T. and Murialdo,H. (1993) Structural transitions during maturation of bacteriophage lambda capsids. *J. Mol. Biol.*, **233**, 682–694.

Dreiseikelmann,B. (1994) Translocation of DNA across bacterial membranes. *Microbiol. Rev.*, **58**, 293–316.

Francki,R.I.B., Fauquet,C.M., Knudson,D.L. and Brown,F. (1991) Classification and nomenclature of viruses. In *Classification and Nomenclature of Viruses.* Springer-Verlag, Wien, Austria, Supplement 2.

Frank,J., Shimkin,B. and Dowse,H. (1981) SPIDER—a modular software system for electron image processing. *Ultramicroscopy*, **6**, 343–358.

Fujisawa,H. and Hearing,P. (1994) Structure, function and specificity of the DNA packaging signals in double-stranded DNA viruses. *Semin. Virol.*, **5**, 5–13.

Fukami,A. and Adachi,K. (1965) A new method of preparation of a self-perforated micro-plastic grid and its application. *J. Electron Microsc. (Japan)*, **14**, 112–118.

Fuller,S.D. (1987) The T=4 envelope of sindbis virus is organized by complementary interactions with a T=3 icosahedral capsid. *Cell*, **48**, 923–934.

Fuller,S.D., Berriman,J., Butcher,S.J. and Gowen,B.E. (1995a) Low pH induces swiveling of the glycoprotein heterodimers in the Semliki Forest virus spike complex. *Cell*, **81**, 715–725.

Fuller,S.D., Butcher,S.J., Cheng,R.H. and Baker,T.S. (1995b) Three-dimensional reconstruction of icosahedral particles—the uncommon line. *J. Struct. Biol.*, in press.

Furcinitti,P.S., van Oostrum,J. and Burnett,R.M. (1989) Adenovirus polypeptide IX revealed as capsid cement by difference images from electron microscopy and crystallography. *EMBO J.*, **8**, 3563–3570.

Greber,U.R., Willetts,M., Webster,P. and Helenius,A. (1993) Stepwise dismantling of adenovirus 2 during entry into cells. *Cell*, **75**, 477–486.

Grimes,J., Basak,A.K., Roy,P. and Stuart,D. (1995) The crystal structure of bluetongue virus VP7. *Nature*, **373**, 167–170.

Ilag,L.L. *et al.* (1995) DNA packaging intermediates of bacteriophage phiX174. *Structure*, **3**, 353–363.

Kotilainen,M.M., Grahn,A.M., Bamford,J.K. and Bamford,D.H. (1993) Binding of an *Escherichia coli* double-stranded DNA virus PRD1 to a receptor coded by an IncP-type plasmid. *J. Bacteriol.*, **175**, 3089–3095.

Lessl,M. and Lanka,E. (1994) Common mechanisms in bacterial conjugation and Ti-mediated T-DNA transfer to plant cells. *Cell*, **77**, 321–324.

Luo,C., Butcher,S. and Bamford,D.H. (1993a) Isolation of a phospholipid-free protein shell of bacteriophage PRD1, an *Escherichia coli* virus with an internal membrane. *Virology*, **194**, 564–569.

Luo,C., Hantula,J., Tichelaar,W. and Bamford,D.H. (1993b) Bacteriophage PRD1 proteins: cross-linking and scanning transmission electron microscopy analysis. *Virology*, **194**, 570–575.

Metcalf,P., Cyrklaff,M. and Adrian,M. (1991) The three-dimensional structure of reovirus obtained by cryo-electron microscopy. *EMBO J.*, **10**, 3129–3136.

Mindich,L. and Bamford,D.H. (1988) Lipid containing bacteriophages. In Calendar,R. (ed.), *The Bacteriophages*. Plenum Press, New York, Vol. 2, pp. 475–520.

Mindich,L., Cohen,J. and Weisburd,M. (1976) Isolation of nonsense suppressor mutants in *Pseudomonas*. *J. Bacteriol.*, **126**, 177–182.

Mindich,L., Bamford,D.H., Goldthwaite,C., Laverty,M. and Mackenzie,G. (1982a) Isolation of nonsense mutants of lipid-containing bacteriophage PRD1. *J. Virol.*, **44**, 1013–1020.

Mindich,L., Bamford,D.H., McGraw,T. and Mackenzie,G. (1982b) Assembly of bacteriophage PRD1: particle formation with wild-type and mutant viruses. *J. Virol.*, **44**, 1021–1030.

Myung,H., Vanden Boom,T. and Cronan,J.E. (1994) The major capsid protein of the lipid-containing bacteriophage PR4 is the precursor of two other capsid proteins. *Virology*, **198**, 17–24.

Olkkonen,V.M. and Bamford,D.H. (1989) Quantitation of the adsorption and penetration stages of bacteriophage phi6 infection. *Virology*, **171**, 229–238.

Olsen,R.H., Siak,J. and Gray,R.H. (1974) Characteristics of PRD1, a

plasmid-dependent broad host range DNA bacteriophage. *J. Virol.*, **14**, 689–699.

Pakula,T.M., Savilahti,H. and Bamford,D.H. (1989a) Comparison of the amino acid sequence of the lytic enzyme from broad-host-range bacteriophage PRD1 with sequences of other cell-wall-peptidoglycan lytic enzymes. *Eur. J. Biochem.*, **180**, 149–152.

Pakula,T.M., Savilahti,H. and Bamford,D.H. (1989b) The organization of the right-end early region of bacteriophage PRD1 genome. *Gene*, **85**, 53–8.

Pansegrau,W. *et al.* (1994) Complete nucleotide sequence of Birmingham IncP alpha plasmids. Compilation and comparative analysis. *J. Mol. Biol.*, **239**, 623–663.

Paredes,A.M., Brown,D.T., Rothnagel,R., Chiu,W., Schoepp,R.J., Johnston,R.E. and Prasad,B.V.V. (1993) Three-dimensional structure of a membrane-containing virus. *Proc. Natl Acad. Sci. USA*, **90**, 9095–9099.

Prasad,B.V.V., Prevelidge,P.E., Marietta,E., Chen,R.O., Thomas,D., King,J. and Chiu,W. (1993) Three-dimensional transformation of capsids associated with genome packaging in a bacterial virus. *J. Mol. Biol.*, **231**, 65–74.

Rey,F.A., Heinz,F.X., Mandl,C., Kunz,C. and Harrison,S.C. (1995) The envelope glycoprotein from tick-borne encephalitis virus at 2Å resolution. *Nature*, **375**, 291–295.

Salas,M. (1991) Protein-priming of DNA replication. *Annu. Rev. Biochem.*, **60**, 39–71.

Savilahti,H. and Bamford,D.H. (1986) Linear DNA replication: inverted terminal repeats of five closely related *Escherichia coli* bacteriophages. *Gene*, **49**, 199–205.

Simons,K. and Fuller,S.D. (1987) The budding of enveloped viruses: a paradigm for membrane sorting? In Burnett,R.M. and Vogel,H.J. (eds), *Biological Organization: Macromolecular Interactions at High Resolution*. Academic Press, Orlando, FL, pp. 139–150.

Stewart,P.L., Burnett,R.M., Cyrklaff,M. and Fuller,S.D. (1991) Image reconstruction reveals the complex molecular organization of adenovirus. *Cell*, **67**, 145–154.

Stewart,P.L., Fuller,S.D. and Burnett,R.M. (1993a) Difference imaging of adenovirus: bridging the resolution gap between X-ray crystallography and electron microscopy. *EMBO J.*, **12**, 2589–2599.

Stewart,P.L., Ghosh,S., Bamford,D.H. and Burnett,R.M. (1993b) Crystallization of the major coat protein of PRD1, a bacteriophage with an internal membrane. *J. Mol. Biol.*, **230**, 349–352.

Varghese,J.N., Laver,W.G. and Colman,P.M. (1983) Structure of the influenza virus glycoprotein antigen neuraminidase at 2.9Å resolution. *Nature*, **303**, 35–40.

Walin,L., Tuma,R., Thomas,G.J. and Bamford,D.H. (1994) Purification of viruses and macromolecular assemblies for structural investigations using a novel ion exchange method. *Virology*, **201**, 1–7.

White,J.M. (1992) Membrane fusion. *Science*, **258**, 917–924.

Wilson,I.A., Skehel,J.J. and Wiley,D.C. (1981) Structure of the haemagglutinin membrane glycoprotein of influenza virus at 3Å resolution. *Nature*, **289**, 366–373.

Received on June 26, 1995; revised on August 30, 1995